

# A Spectral Element Ocean Model on the Cray T3D: the Interannual Variability of the Mediterranean Sea General Circulation

A. J. Molcard, N. Pinardi<sup>1</sup> and R. Ansaloni<sup>2</sup>

<sup>1</sup>Istituto per lo Studio delle Metodologie Geofisiche Ambientali, Bologna, Italy

<sup>2</sup>Silicon Graphics S.p.A., Milano, Italy

Received 25 April 1997; accepted 26 September 1997

**Abstract.** A new numerical model, SEOM (Spectral Element Ocean Model, (Iskandarani et al, 1994)), has been implemented in the Mediterranean Sea. Spectral element methods combine the geometric flexibility of finite element techniques with the rapid convergence rate of spectral schemes. The current version solves the shallow water equations with a fifth (or sixth) order accuracy spectral scheme and about 50,000 nodes. The domain decomposition philosophy makes it possible to exploit the power of parallel machines. The original MIMD master/slave version of SEOM, written in F90 and PVM, has been ported to the Cray T3D. When critical for performance, Cray specific high-performance one-sided communication routines (SHMEM) have been adopted to fully exploit the Cray T3D interprocessor network. Tests performed with highly unstructured and irregular grid, on up to 128 processors, show an almost linear scalability even with unoptimized domain decomposition techniques. Results from various case studies on the Mediterranean Sea are shown, involving realistic coastline geometry, and monthly mean 1000mb winds from the ECMWF's atmospheric model operational analysis from the period January 1987 to December 1994. The simulation results show that variability in the wind forcing considerably affect the circulation dynamics of the Mediterranean Sea.

© 1998 Elsevier Science Ltd. All rights reserved

## 1 Introduction

In this paper we present the implementation in the Mediterranean area of a new numerical model for the simulation of the general circulation of the basin. The Mediterranean Sea has a complicated coastline geometry with intense dynamical interactions between continental margin areas and open ocean regions. Therefore, a variable resolution, high accuracy numerical model is

desirable. The spectral element technique allows a flexible representation of the domain and a higher accuracy than traditional numerical methods. Spectral element techniques are also particularly appropriate for implementation on parallel machines mainly due to the possibility of carrying out large computations within each element and few inter-processor communications.

## 2 Spectral Element model

### 2.1 Dynamical equations

The model solves the shallow water equations with full or reduced gravity in the rotating frame. Two momentum and one continuity equations are solved for the three unknowns, sea surface elevation ( $\zeta$ ), zonal and meridional velocities ( $\mathbf{u}=(u,v)$ ).

The shallow water equations are:

$$\begin{aligned} \mathbf{u}_t + \mathbf{u} \cdot \nabla \mathbf{u} + f \hat{\mathbf{k}} \times \mathbf{u} + g \nabla \zeta - \frac{\nabla \cdot [\nu(h + \zeta) \nabla \mathbf{u}]}{(h + \zeta)} \\ = \frac{\tau}{\rho(h + \zeta)} - \frac{\gamma}{h + \zeta} \mathbf{u} \end{aligned}$$

$$\zeta_t + \nabla \cdot [(h + \zeta) \mathbf{u}] = 0$$

$\hat{\mathbf{k}}$  is a unit vector in the vertical direction;  $h$ , the resting depth of the fluid;  $f = f_0 + \beta_0 y$ , where  $\beta_0 = 2\Omega \cos \Theta_0$  and  $\Theta_0 = 37^\circ$  and  $\Omega = 7,310^{-5}$  rad/s;  $g$  the gravitational acceleration;  $\gamma$ , the bottom drag coefficient,  $\nu$ , the diffusion coefficient;  $\rho$ , the constant density of the fluid;  $\tau = (\tau^x, \tau^y)$ , the wind stress acting on the surface of the fluid; and  $\nabla$ , the two-dimensional gradient operator. The subscript  $t$  denotes differentiation with respect to time. We impose no slip boundary conditions at lateral walls and  $\gamma$ ,  $\tau$ ,  $\rho$  and  $\nu$  are given.

Correspondence to: A. Molcard

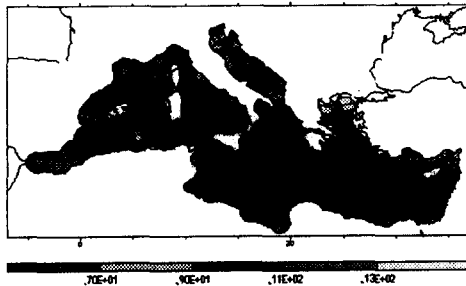


Fig. 1. Distribution of spectral elements: the greyscale bar represents the average grid spacing (km) in each element

## 2.2 Numerical method

In the spectral element discretization the domain is broken up into quadrangular elements and the dependent variables (velocity and pressure) are approximated by high order polynomial expansions within each element. A judicious choice of the interpolation polynomial and of the integration rule can reduce substantially the amount of memory and CPU needed to store and invert the system of equations. Legendre Cardinal functions are chosen for the interpolation and Gauss-Lobatto quadrature for the integration. We use a staggered grid to avoid spurious pressure modes that could destroy the solution and the pressure is interpolated with a polynomial of degree two less than that used for the velocity. The grids are built in order to better resolve the geometrical coastline constraints: small elements are used in important regions where complex dynamical phenomena occurs (Gibraltar and Sicily straits, Gulf of Lions) whilst regional basins such as the Adriatic and Aegean Sea are left coarsely resolved (see an example of a spectral element grid in Fig. 1).

The time integration is done by an explicit third-order Adams-Bashforth scheme. This integration method is only conditionally stable, the most severe stability limit being dictated by the speed of the free surface gravity waves. At sub-element level, the spectral finite element method is algorithmically analogous to the spherical harmonic approach used in atmospheric models. At the level of individual elements, information exchange is between neighbours only, as is typical for the low order schemes used in traditional ocean circulation models.

Spectral Element Methods allow a flexible representation of complex geometry and high accuracy but could become an huge computational problem when modelling global ocean circulation. As simulations become more realistic, the computational power required to produce them grows rapidly. Parallel processing (two or more processor nodes, each executing logical parts of a program simultaneously) makes it possible to get the most out of available computational power. Since the sharing of information is sparse across the element boundaries, the Spectral Element model maps naturally and efficiently onto high performance parallel computer architectures.

## 3.1 Porting

The original version of SEOM was written in Fortran 90 for a MIMD parallel machine with a master/slave paradigm using PVM library routines for interprocessors communication. This means that a master processor controls the activity of a group of slave processors, assigning the work to be done in parallel and taking care of the I/O operations (e.g. reading the grid or periodically writing output informations). When porting the code to the Cray T3D a different approach must be used and a substantial rewriting of the code was necessary. The master/slave paradigm cannot be easily implemented on the Cray T3D since a processor cannot spawn processes on other processors and the best possible implementation consists in having a processor to play both master and slave roles. In a few critical points the traditional message-passing (PVM) have been replaced by Cray proprietary high-performance one-sided routines (SHMEM). These routines allow to exploit the hardware feature of the Cray T3D that enables each processor to access directly the memory of another processor without involving that remote processor: this is possible because the T3D network operates independently of the processors.

## 3.2 Performance

A small test case (100 iterations with a constant wind forcing) has been defined to analyse the performance of the code and to compare it with runs on other systems. In the literature a great importance is usually ascribed to the quality of the decomposition algorithm used to distribute the grid across the processors. Thus two different decompositions are compared with SHMEM and PVM routines. A default decomposition (def experiment) is done directly in the code, assigning the elements to the processors in the order they are read in. No optimization takes place to minimize communication. As the grid has been generated by blocks, neighbouring elements may not have sequential index-

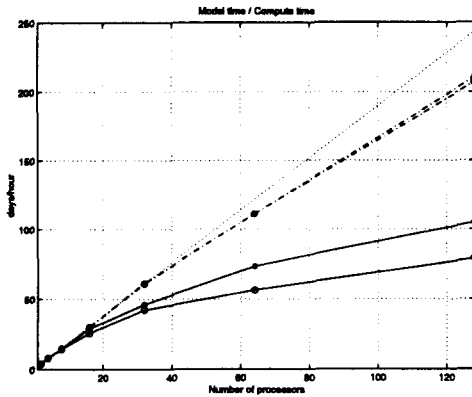


Fig. 2. Performance of the program depending on the decomposition (def(circle) and BFS(star)) and the communication (PVM(solid line) and SHMEM(dashdot line)) routine in terms of simulated days per computed hour. The dotted line represents the ideal linear scalability.

ing, and thus the code could generate inefficient communication paths. Another, more sophisticated decomposition (BFS experiment) scheme is used, based on a Breath First Search tree spanning algorithm (Kruse, 1987). This scheme decomposes the grid trying to minimize the perimeter-to-area ratio of each domain thus increasing the computational load per domain.

The performance is measured by the functions  $S(p)$  which represents the number of days simulated in an hour of compute time (Hockney, 1996): it is thus a speed-like function of the kind (where  $T(p)$  is the compute time with  $p$  processors):

$$S(p) = (1/24) \times \text{simulated.time} / T(p).$$

Fig. 2 shows the importance of the mapping among all processors when using the traditional message passing (PVM). The number of collocation points that are shared between processors (where information has to be exchanged) will be proportional to the perimeter length of the domain in each processor. In the default decomposition case (def\_PVM) where no optimization takes place, some distant parts of the domain could be attributed to the same processor and the total cost of communication will increase drastically with the processor number. In this case an optimal mapping (BFS\_PVM) is necessary: optimal load-balancing is obtained and the time lost in communication is reduced. This version of the code does not appear to be very efficient on the Cray T3D. Using SHMEM communications routines, instead of PVM, in a small but critical routine where neighbour processors exchange border data, it is possible to exploit the low latency features of the interprocessor network. Now the time lost in communication is reduced and is irrelevant in comparison with the computational operation time. In this case the choice of the data decomposition is not important (BFS versus def).

## 4 Results

Circulation processes in the Mediterranean Sea are dynamically rich, and include quasi-permanent sub-basin-scale gyres, an intense mesoscale eddy fields and a seasonally varying general circulation. From the work of Moskalenko (Moskalenko, 1974), Heburn (Heburn, 1987), Malanotte-Rizzoli and Bergamasco (Malanotte-Rizzoli *et al.*, 1991), Pinardi and Navarra (Pinardi *et al.*, 1993) it is well known that winds and wind stress curl are the major driving mechanism of the basin scale gyres. The seasonal character of the circulation and its interannual variabilities have started to emerge only recently from the most recent data, especially collected in the Eastern Mediterranean (Robinson *et al.*, 1992; Horton *et al.*, 1994). Our investigation aims to the understanding and simulation of the interannual variability of these structures due to the eddy-mean flow interactions that may occur and that by itself could modify the flow field independently from atmospheric forcing. Thus our major scientific questions are:

- 1) which part of the seasonal/interannual variability of the flow field is driven by atmospheric anomalies?
- 2) which part is instead due to nonlinear equilibria in the basin?
- 3) what is the direction of the eddy-mean flow interactions in the basin and what is the energetic of basin scale gyre interactions?

In order to answer these questions we needed an accurate numerical model and accurate atmospheric forcings. The study of the simulations has just only started but some relevant results are already evident.

### 4.1 Model design

The wind-driven component of the circulation in the Mediterranean Sea is analysed by means of the free-surface primitive equation reduced gravity model previously described and implemented on a Cray T3D or T3E. The reduced gravity model is designed to represent the first internal mode and contains an upper active layer and a lower layer which is infinitely deep and at rest. Consequently, bottom topography and baroclinic instability are not permitted.  $\zeta$  represents now the interface displacement instead of the surface elevation in the full gravity simulations. Since the gravity constant is much smaller than in the full gravity, we could increase the time step significantly.

This design is applied with a spectral grid containing 681 elements, and uses a 6th order accuracy scheme (see Fig. 1). The model was driven by monthly mean 1000mb winds from the ECMWF's atmospheric model operational analysis from the period January 1987 to December 1994. This forcing was computed from the original six hour data set which was at an horizontal resolution of  $0.5625^\circ$ . The monthly averages were bilinearly interpolated in space to the spectral grid and

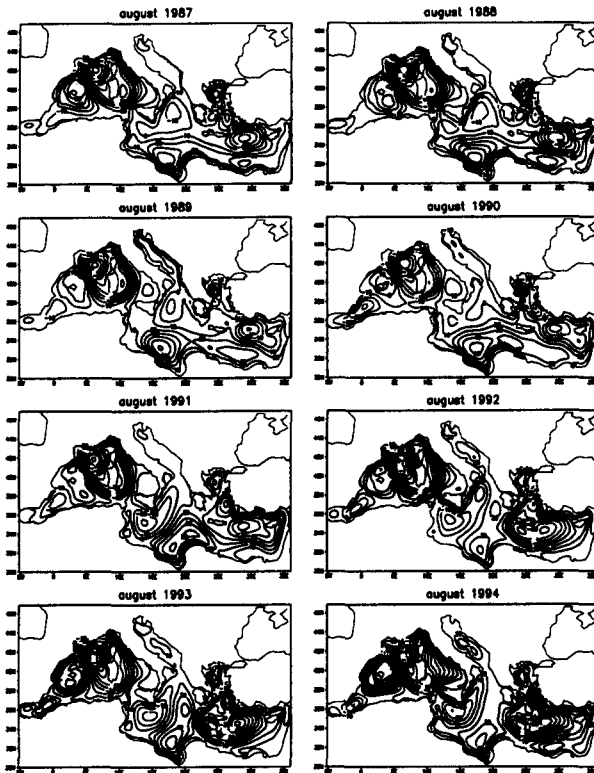


Fig. 3. Snapshot of interface displacement (m) for august from 1987 to 1994

linearly interpolated in time at each model time step. When analysing the winds, a strong seasonal and inter-annual variability appeared with different wind regimes prevailing in the Eastern and Western parts of the basin. The stress field is characterised by two prominent features that persist throughout the seasons and the years, but can change substantially in intensity: the Mistral wind over the Western Mediterranean blowing through the gap between the Pyrenees and the Alps and the Etesian regime over the Eastern Mediterranean.

#### 4.2 Simulation results

The simulation results show most of the known sub-basin gyres. Fig. 3 depicts the pycnocline height for august from 1987 to 1994 in the Mediterranean basin. The dominant features of the circulation in the Western Mediterranean are the large persistent cyclonic gyres in the Provençal and Thyrrenian basins under the influence of the northwesterly flow in the climatological wind fields. An anticyclonic circulation is also present in the Balearic Sea corresponding to a wind stress curl centre present throughout the years. The structure of the Eastern Mediterranean is more complicated and presents sub-basin scale features and boundary and open ocean

jet currents. Examples of these are: the Mid-Mediterranean Jet and the Ionian-Atlantic current; the cyclonic Rhodes gyre (corresponding to the wind stress curl centre placed north east of Rhodes island) and a Cretan cyclone on the southwest side of Crete. Some small anticyclonic eddy-like features appear south of Cyprus, that composed the Shikmona gyre system (Ozsöy, 1989). If we focus on the so-called Mersa-Matruh gyre in the Levantine basin (the anticyclonic gyre centered about  $25^{\circ}$ - $28^{\circ}$ ), it is evident that it weakens and shrinks considerably starting from 1990. This result may be thought to agree with the two data sets collected in the Eastern Mediterranean, one in 1987 (Robinson *et al.*, 1992), where a strong anticyclonic gyre was present during the cruise and was considered as permanent, and the other in 1992 (Horton *et al.*, 1994), where the Mersa-Matruh subgyre system was a collection of weaker anticyclones. Our results generally indicate that wind stress variability is responsible for major changes in circulation structures.

#### 5 Conclusions

The Spectral Element Ocean Model used in this work, permits flexible representation of complex geometry, regional mesh refinement, exponential convergence, high accuracy, and a nearly perfect scalability on parallel computers. All these reasons suggest that this kind of numerical techniques, even if more complex than traditional schemes (finite differences) can be very efficient on parallel machines like the T3D. This model has been used to study the wind-driven circulation on the Mediterranean Sea and when forcing the model with realistic wind stresses, an evident seasonal and interannual variability emerged.

*Acknowledgements.* A. Molcard and N. Pinardi were supported by the EU-MAST (contract MAS2-CT94-5017) and MATER-MTP (contract MAS3-CT96-0051). All the simulations were run on the Cray T3D and T3E at CINECA, Italy. The initial code was kindly supplied by Dr. Iskandarani of Rutgers University.

#### References

- Haidvogel D.B., Curchister, E., Iskandarani, M., Hugues, R., Global modeling of the Ocean and the Atmosphere using the spectral element method, submitted to *Atmosphere-Ocean*, 1995.
- Heburn, G.W., The dynamics of the western Mediterranean Sea: a wind forced cast study, *Annales Geophysicae*, 5B(1), 61-74, 1987.
- Hockney, R.W., The Science of Computer Benchmarking, SIAM, Philadelphia, 1996.
- Horton, C., Kerling, K., Athey, G., Schmits, J., Clifford, M., Airborne expendable bathythermograph surveys of the eastern Mediterranean, *Journal of Geophysical Research*, 99(C5), 9891-9905, 1994.
- Iskandarani, M., Haidvogel, D.B. and Boyd, J.P., A staggered spectral finite element model with application to the oceanic shallow water equations, *Int. J. Num. Meth. Fl.*, 20, 393-414, 1994.

- Kruse, R., *Data Structures and Program Design*, Prentice Hall, New York, 1987.
- Malanotte-Rizzoli, P. and Bergamasco, A., The wind and thermally driven circulation of the Eastern Mediterranean, *Dynamics of Atmospheres and Oceans*, 12(4), 335-351, 1989.
- Moskalenko, L.V., Steady-state Wind-driven currents in the Eastern part of the Mediterranean Sea, *Okeanologiya*, 14(4), 491-494, 1974.
- Ozsöy, E., Hecht, A., Ünlüata, Ü., Circulation and hydrography of the Levantine basin: results of POEM coordinated experiments 1985-1986, *Progress in Oceanography*, 22, 125-170.
- Pinardi, N., Navarra, A., Baroclinic adjustment processes in the Mediterranean Sea, *Deep-Sea Research*, 40(6), 1299-1326, 1993.
- Robinson, A.R, et al, General circulation of the Eastern Mediterranean, *Earth-Science Reviews*, 32, 285-309, 1992.